RSC Advances

PAPER

View Article Online
View Journal | View Issue

Cite this: *RSC Adv.*, 2017, **7**, 56211

Atmospheric chemistry of CH_3O: its unimolecular reaction and reactions with H_2O, NH_3, and HF†

Mei-Ling Wei,‡[a] Xing-Feng Tan,‡[b] Zheng-Wen Long*[a] and Bo Long *[ab]

We have investigated the hydrogen atom transfer processes of CH_3O to CH_2OH without catalyst and with water, ammonia, and hydrofluoric acid as catalysts using *ab initio* methods, density functional theory (DFT) methods, and canonical variational transition state theory with small curvature tunneling (CVT/SCT). Herein, we have performed the benchmark barrier heights of the title reactions using W3X-L//CCSD(T)-F12a/VDZ-F12 methods. We have also performed the calculations of the combination of MPW-type, PBE-type exchange, M05-type, M06-type functional, and composite theoretical model chemistry methods such as CBS-QB3 and G4. We found that the M05-2X/aug-cc-pVTZ, mPW2PLYP/MG3S, M05-2X/aug-cc-pVTZ, and M06-2X/MG3S methods are performed better in different functionals with the unsigned errors (UEs) of 0.34, 0.02, 0.05, and 0.75 kcal mol^{-1} for its unimolecular reaction and reactions with H_2O, NH_3, and HF, respectively. The calculated results show that NH_3 exerts the strongest catalytic role in the isomerization reaction of CH_3O to CH_2OH, compared with H_2O and HF. In addition, the calculated rate constants show that the effect of tunneling increases the rate constant of the unimolecular reaction of CH_3O by 10^2–10^{12} times in the temperature range of 210–350 K. Moreover, the variational effects of the transition state are obvious in $CH_3O + NH_3$. The calculated results also show that the direct unimolecular reaction of CH_3O to CH_2OH is dominant in the sink of CH_3O, compared with the $CH_3O + H_2SO_4$, CH_3O + HCOOH, $CH_3O + H_2O$, $CH_3O + NH_3$, and CH_3O + HF reactions in the atmosphere. The present results provide a new insight into catalysts that not only affect energy barriers, but have influences on tunneling and variational effects of transition states. The present findings should have broad implications in computational chemistry and atmospheric chemistry.

Received 19th August 2017
Accepted 6th December 2017

DOI: 10.1039/c7ra09167b

rsc.li/rsc-advances

1. Introduction

Alkoxy radicals have received a great amount of attention because they play a key role in both combustion and atmospheric chemistry.[1] The methoxy radical (CH_3O) is one of the simplest alkoxy radicals.[2] CH_3O is produced from OH-initiated oxidation of CH_4.[2] In the atmosphere, CH_3O undergoes unimolecular isomerization and decomposition and bimolecular reaction.[1] While CH_3O dominantly reacts with O_2, responsible for the formation of HCHO and HO_2, the $CH_2OH + O_2$ reaction is 10^4 times faster than the $CH_3O + O_2$ reaction, where CH_2OH is formed through the hydrogen atom transfer of CH_3O.[3–5] Therefore, Radford stated that the isomerization reaction of CH_3O could be an important process for the loss of CH_3O.[6] Exploring the unimolecular isomerization of CH_3O is required to estimate the fate of CH_3O in the atmosphere.

The reaction kinetics and dynamics of methoxy radicals (CH_3O) has been extensively investigated for both experimental and theoretical methods in the literature.[1,7–19] However, the kinetics of the unimolecular isomerization reaction of CH_3O remains unclear. With regard to the unimolecular reaction of CH_3O, the energy barrier is very high, in the range of 26–36 kcal mol^{-1}, depending on different theoretical methods.[14,16,20–22] For example, Batt *et al.*[16] estimated an energy barrier of 26.1 kcal mol^{-1}, Tachikawa *et al.*[22] reported an energy barrier of 32.88 kcal mol^{-1} calculated by CCSDST4/D95V**, Saebo *et al.*[14] reported an energy barrier of 36 kcal mol^{-1} calculated by MP3/6-31G**. This uncertainty of energy barrier of CH_3O unimolecular isomerization leads to the difficulty in quantitatively estimating the rate constant of CH_3O unimolecular isomerization reaction. In addition, CH_3O unimolecular isomerization is a hydrogen atom transfer (HAT) reaction. In particular, tunneling effects play a critical role in reaction kinesics for hydrogen transfer reactions,[23,24] such as the unimolecular reactions of Criegee intermediates,[25–28] $CH_3OH + OH$,[29] $OH + H_2SO_4\cdots NH_3$,[30] unimolecular rearrangement of $Rh(PH_3)_2ClCH_4$,[31] H/D + CO,[32,33] H/D + CH_3OH,[34] and Al

[a]*Department of Physics, Guizhou University, Guiyang, 550025, China. E-mail: zwlong@gzu.edu.cn*

[b]*College of Material Science and Engineering, GuizhouMinzu University, Guiyang, 550025, China. E-mail: longbo@gzmu.edu.cn; wwwltcommon@sina.com*

† Electronic supplementary information (ESI) available: Table S1 listing barrier heights at different theoretical methods and Table S2 providing Cartesian coordinates. See DOI: 10.1039/c7ra09167b

‡ Mei-Ling Wei and Xing-Feng Tan contributed equally.

+ $3H_2O$.[35] Therefore, it is necessary to reevaluate kinetics of the unimolecular isomerization reaction of CH_3O.

The other issue is that there are some reports that water and atmospheric acids can remarkably decrease the energy barrier of hydrogen atom transfer reaction.[36] More over water, sulfuric acid, and formic acid have been reported as catalysts to reduce the isomerization of methoxy to 25.7, 2.3, and 4.2 kcal mol^{-1}, respectively.[36] In particular, the calculated results are 25.7 kcal mol^{-1} by Buszek *et al.*[36] and 22.9 kcal mol^{-1} by Kumar *et al.*[5] at the CCSD(T)/aug-cc-pVTZ//QCISD/6-31G(d) and CCSD(T)/aug-cc-pVTZ//MP2/aug-cc-pVTZ, respectively. It is noted that the reported water catalytic CH_3O isomerization of the energy barrier has difference of 2–3 kcal mol^{-1}. This results lead to the inaccuracy of evaluating the kinetics of the methoxy unimolecular isomerization reaction. In addition, the catalytic effect of ammonia is better than water in the literature.[37] Hydrofluoric acid is an important inorganic acid in the atmosphere. So, we calculated the H_2O, NH_3, and HF as catalysts in the unimolecular isomerization reaction of CH_3O.

In this work, we investigated the hydrogen atom transfer processes of CH_3O to CH_2OH catalyzed by water, ammonia, and hydrofluoric acid using *ab initio* methods and density functional theory (DFT) methods, and canonical variational transition state theory with small curvature tunneling (CVT/SCT). We studied following reactions:

$$CH_3O \rightarrow CH_2OH \quad (1)$$

$$CH_3O + M \rightarrow CH_2OH + M \quad (2)$$

where M stands for H_2O, NH_3, and HF. The purpose of this work is to determine which functional is best for every specific reaction studied here and estimate the catalytic capability of these catalysts, explore the tunneling effects, and obtain the quantitative rate constants. Herein, we also present definitive examples how to use theoretical methods to predict the quantitative rate constants for hydrogen atom transfer reactions.

2. Computational methods

2.1. Benchmark calculation

It is of great necessity for studying the atmospheric reactions with high-accurate electronic structure methods to obtain quantitative results. We used the CCSD(T)-F12a/VDZ-F12 (ref. 38–40) and QCISD/VTZ[41] methods for optimizing the reactants, pre-reactive complexes, transition states, post-reactive complexes, and products and calculating their corresponding frequencies. Single point energy calculations were carried out using the W2X[42] and W3X-L[42] methods at the CCSD(T)-F12a/VDZ-F12 and QCISD/VTZ optimized geometries, respectively. We have obtained the benchmark barrier heights of hydrogen atom transfer reactions for CH_3O to CH_2OH by different catalysts at the W3X-L//CCSD(T)-F12a/VDZ-F12 level as our best estimate. It is worth noting that W3X-L composite methods have been used in the reactions of Criegee intermediates with water,[25] SO_2 with OH,[43] and HO_2 with XCHO[44] to obtain rate constants with experimental accuracy.

2.2. Composite method calculation

Quantum chemical composite methods have developed because they approaches CCSD(T)/CBS.[45] We used G4,[45] unrestricted coupled cluster spin contamination corrected [UCCSD(T)], and unrestricted Brueckner doubles [UBD(T)] variations of the Weizmann-1 theory (W1), named as W1U and W1BD,[46] and the CBS-QB3 (ref. 47) method.

2.3. Density functional theory (DFT) calculation

We studied different functionals: (1) the generalized gradient approximation (GGA) such as B98 ref. 48) and BP86 (ref. 49–51; (2) depending on the density of Laplace or kinetic energy density of meta-GGA such as M11-L;[52] (3) hybrid GGA with the addition of Hartree–Fock (HF) exchange to non-local information of occupied orbital such as BMK,[53] HSEh1PBE,[54–57] MPW1K,[58–60] and MPW3LYP;[61] (4) global-hybrid meta-GGA: B3LYP,[62] M05-2X,[63] M06-HF,[64] and M06-2X;[65] (5) range-separated hybrid meta GGA such as M11 (ref. 66) and range-separated meta-NGA such as MN12-SX;[67] (6) double hybrid density functional using from both occupied and virtual orbital such as B2PLYP,[68] B2PLYPD,[69] and mPW2PLYP.[70] These computations were finished using aug-cc-pVTZ,[71–73] maug-cc-pVTZ,[74] MG3S,[75] and ma-TZVP[76] basis sets.

2.4. Reaction kinetics

The rate constants were calculated using canonical variational transition-state theory with small curvature tunneling (CVT/SCT).[77–81] We selected the best functional for every specific reactions to do direct dynamics calculations by comparing with our best estimate. The unimolecular rate constants of CH_3O to CH_2OH was calculated by M05-2X/aug-cc-pVTZ, while the bimolecular rate constants of the CH_3O + H_2O, CH_3O + NH_3, and CH_3O + HF reactions were calculated using mPW2PLYP/MG3S, M05-2X/maug-cc-pVTZ, and M06-2X/MG3S, respectively. Scale factors[82] were used to scale all directly calculated harmonic vibrational frequencies, which are 0.964, 0.972, 0.964, and 0.970 for M05-2X/aug-cc-pVTZ, mPW2PLYP/MG3S, M05-2X/maug-cc-pVTZ, and M06-2X/MG3S, respectively.

The optimization and frequency calculations of all geometries including reactants, transition states, and products calculated were carried out with the Gaussian 09 (ref. 83) suites of programs. The high level geometry optimization calculations are performed using the Molpro 2012 (ref. 84) suites of programs. Rate constants were calculated using the Polyrate 2010A[85] and Gaussrate 2009 (ref. 86) dynamics codes.

3. Results and discussion

We have obtained the benchmark barrier heights of CH_3O to CH_2OH without catalyst and with water, ammonia, and hydrofluoric acid as catalysts using W3X-L//CCSD(T)-F12a/VDZ-F12 methods. We defined the unsigned error (UE) to determine which is the best functional, and UE is the absolute value of the difference between the computed barrier heights by different methods and the benchmark barrier heights calculated by W3X-L//CCSD(T)-F12a/VDZ-F12.

3.1. The unimolecular isomerization of CH_3O

The unimolecular isomerization of CH_3O into CH_2OH occurs *via* the transfer of the hydrogen atom of CH_3 group to the oxygen atom in CH_3O responsible for the formation of CH_2OH as shown in Fig. 1. The unimolecular isomerization of CH_3O into CH_2OH has been extensively studied using different theoretical methods; the previous calculated results indicated that the barrier heights of the unimolecular isomerization of CH_3O into CH_2OH are varies between 26.1 and 36.0 kcal mol^{-1}.[14,16,20–22] Therefore, higher-level theoretical methods are required to obtain quantitative results. Herein, we use the benchmark calculation of beyond-CCSD(T) to obtain reliable results. The main results are summarized in Table 1 and Fig. 1, while all the results are provided in Table S1 (ESI).† The calculated results by W3X-L//CCSD(T)-F12a/VDZ-F12 indicate that the barrier height of the reaction is 29.56 kcal mol^{-1} in Table 1. Fig. 2 shows that the results are calculated by various density functional methods and *ab initio* methods, where the UEs are 0.13, 0.18, 0.32, and 0.34 kcal mol^{-1} using W1U, CBS-QB3, W1BD, and M05-2X/aug-cc-pVTZ, respectively; this results reflect slight changes for different theoretical methods. Therefore, the barrier height of the unimolecular isomerization of CH_3O into CH_2OH is computed to be 29.56 kcal mol^{-1} (W3X-L//CCSD(T)-F12a/VDZ-F12), which should be reliable. The W2X//CCSD(T)-F12a/VDZ-F12 result is 29.64 kcal mol^{-1}, which agrees well with the value of 29.56 kcal mol^{-1}; this shows that the electronic

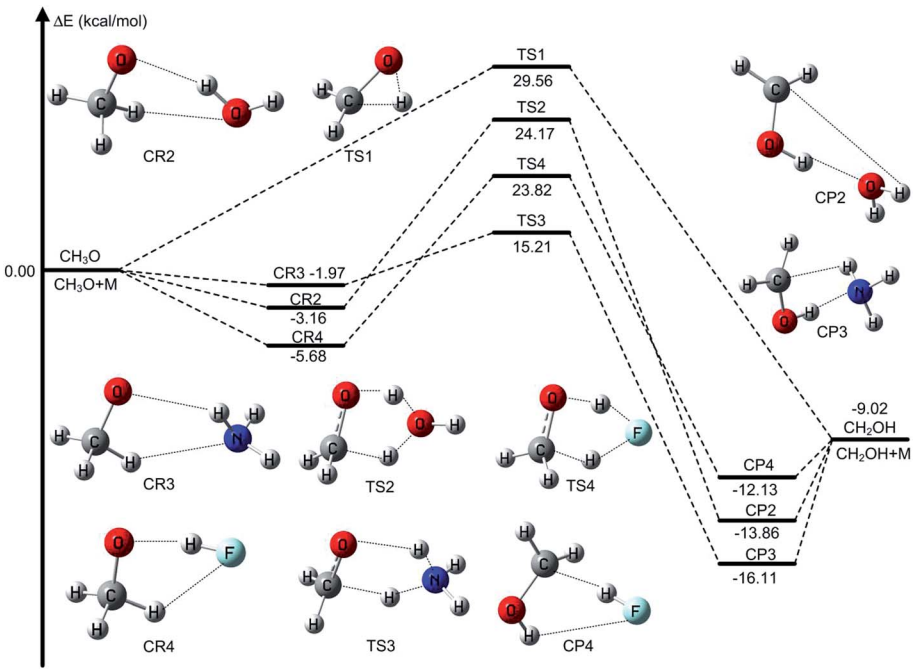

Fig. 1 Variation in potential energy surface for the reactants, intermediates, transition states, and products of the CH_3O isomerization into CH_2OH in the without catalysis and catalyzed by water, ammonia, and hydrofluoric acid reactions at the W3X-L//CCSD(T)-F12a/VDZ-F12 level.

Table 1 The energy barriers of the CH_3O isomerization into CH_2OH, the $CH_3O + H_2O$, $CH_3O + NH_3$, and CH_3O + HF reactions with zero-point energy involved at 0 K (kcal mol^{-1})[a]

Methods	TS1	UE	TS2	UE	TS3	UE	TS4	UE
W3X-L//CCSD(T)-F12a/VDZ-F12	29.56	0.00	24.17	0.00	15.21	0.00	23.82	0.00
W2X//CCSD(T)-F12a/VDZ-F12	29.64	0.08	24.26	0.09	15.26	0.05	24.30	0.48
W2X//QCISD/cc-pVTZ	29.07	0.49	23.82	0.35	14.65	0.56	23.86	0.04
W3X-L//QCISD/cc-pVTZ	28.99	0.57	23.74	0.43	14.62	0.59	23.32	0.50
W1U	29.69	0.13	24.72	0.55	15.32	0.11	25.39	1.57
W1BD	29.88	0.32	24.88	0.71	15.47	0.26	25.11	1.29
mPW2PLYP/MG3S	31.33	1.77	24.15	0.02	15.48	0.27	22.92	0.90
M06-2X/MG3S	30.39	0.83	23.19	0.98	15.71	0.50	23.07	0.75
G4	30.09	0.53	25.87	1.70	15.97	0.76	25.55	1.73
CBS-QB3	29.74	0.18	25.24	1.07	15.06	0.15	27.62	3.80
M05-2X/aug-cc-pVTZ	29.90	0.34	21.35	2.82	15.16	0.05	20.41	3.41
M05-2X/maug-cc-pVTZ	30.04	0.48	21.65	2.52	15.40	0.19	20.80	3.02

[a] Unsigned error (UE) obtained *via* the absolute value of the difference between the computed barrier heights and the benchmark barrier heights.

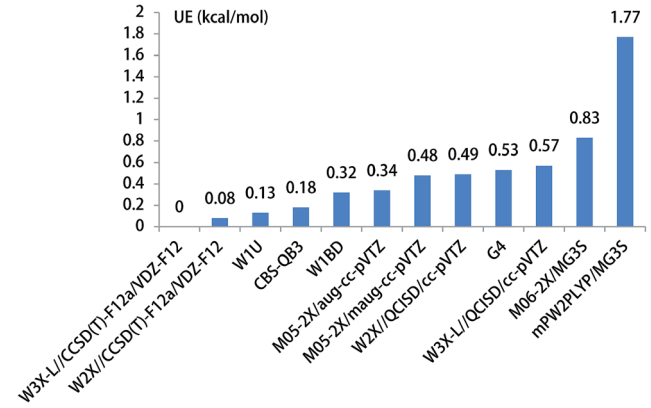

Fig. 2 The unsigned error for the energy barrier of unimolecular isomerization reaction of CH_3O to CH_2OH.

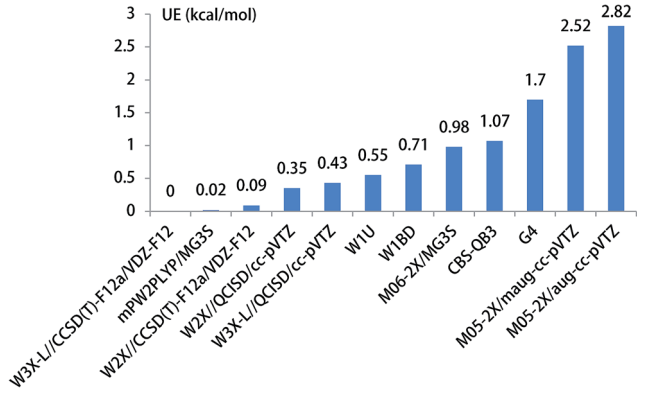

Fig. 3 The unsigned error for the energy barrier of $CH_3O + H_2O$.

structures in the unimolecular reaction of CH_3O to CH_2OH do not represent a multireference character. Additionally, Table 1 shows that the barrier height of CH_3O to CH_2OH by W3X-L//QCISD/cc-pVTZ is calculated to be 28.99 kcal mol^{-1}, which is 0.57 kcal mol^{-1} different from the value (29.56 kcal mol^{-1}) calculated by W3X-L//CCSD(T)-F12/VDZ-F12; this result shows that the optimized geometries and calculated frequencies at the QCISD/cc-pVTZ are in adequate agreement with CCSD(T)-F12a/VDZ-F12 results, which has been observed in the SO_2 + OH reaction,[43] while the QCISD/cc-pVTZ-optimized geometries and calculated frequencies are reliable in the reactions of Criegee intermediates with H_2O.[25] Since the unimolecular reaction of CH_3O to CH_2OH and the SO_2 + OH reaction are open-shell systems, the reliability of QCISD-optimized geometries and calculated frequencies for open-shell systems should be particular concerned to obtain quantitative results in competition with experimental accuracy with an error bar of 0.1–0.2 kcal mol^{-1}.

3.2. The bimolecular reactions of CH_3O with H_2O, NH_3, and HF

The unimolecular isomerization of CH_3O into CH_2OH catalyzed by H_2O, NH_3, and HF occurs *via* the prereactive complex before the corresponding transition state and subsequently undergo the postreactive complex responsible for the formation of CH_2OH as shown in Fig. 1. For example, when water acts as a catalyst, the hydrogen atom of CH_3O is transferred to the oxygen atom in H_2O and simultaneously the hydrogen atom of H_2O is transferred to the terminal oxygen atom in CH_3O responsible for the formation of CH_2OH. The recent investigations have indicated that the energy barrier with water catalysis is 25.7 (ref. 36) and 22.9 (ref. 22) kcal mol^{-1} at the CCSD(T)/aug-cc-pVTZ//QCISD/6-31G(d) and CCSD(T)/aug-cc-pVTZ//MP2/aug-cc-pVTZ, respectively, which is 2.8 kcal mol^{-1} difference between the CCSD(T)/aug-cc-pVTZ//QCISD/6-31G(d) and CCSD(T)/aug-cc-pVTZ//MP2/aug-cc-pVTZ calculated results; this reflects that higher-level theoretical methods are necessary to obtain reliable results. Thus, we calculate the energy barrier of the unimolecular isomerization of CH_3O into CH_2OH with water as a catalyst usingW3X-L//CCSD(T)-F12a/VDZ-F12 theoretical method. The computed energy barrier is 24.17 kcal mol^{-1} in Table 1. Additionally, Fig. 3 shows that the UEs are 0.02, 0.55, and 0.71 kcal mol^{-1} for the mPW2PLYP/MG3S, W1U, and W1BD theoretical methods, respectively, comparing with the barrier height of TS2 calculated by W3X-L//CCSD(T)-F12a/VDZ-F12.

Previous investigations have shown that ammonia has remarkably catalytic role in hydrogen transfer processes in the $H_2SO_4\cdots NH_3$ + OH,[30] $CF_3OH + NH_3$,[37] $SO_3 + H_2O + NH_3$ (ref. 87) reactions. Herein, we investigate the $CH_3O + NH_3$ reaction, resulting in the formation CH_2OH and NH_3, where NH_3 is acted as a catalyst. The optimized geometries of the transition state TS3 are provided in Fig. 1. The energy barrier of the $CH_3O + NH_3$ reaction is 15.21,15.26 kcal mol^{-1} using the best W3X-L//CCSD(T)-F12a/VDZ-F12 method, W2X//CCSD(T)-F12a/VDZ-F12 method in Table 1, which shows that the beyond-CCSD(T) calculations are not necessary for obtain quantitative results; this shows that there are not multireference features in the $CH_3O + NH_3$ reaction. In addition, the QCISD-optimized geometries and frequency calculations are still not adequate accurate to obtain quantitative results because the UE of W3X-L//QCISD/VTZ is 0.59 kcal mol^{-1}, comparing with the results calculated by W3X-L//CCSD(T)-F12a/VDZ-F12 in Table 1. The calculated results also shows that NH_3 has much stronger catalytic ability in the isomerization reaction of CH_3O to CH_2OH than H_2O because the energy of the $CH_3O + NH_3$ reaction is about 9 kcal mol^{-1} lower than that of the $CH_3O + H_2O$ reaction, which also agree with the previous investigation in the $CF_3OH + NH_3$ reaction.[37] It is noted the UE of M05-2X/aug-cc-pVTZ is only 0.05 kcal mol^{-1} in Table 1 and Fig. 4. Thus, the M05-2X/aug-cc-pVTZ theoretical method is chosen to do direct dynamics calculations in the $CH_3O + NH_3$ reaction.

When HF is acted as a catalyst in the CH_3O + HF reaction responsible for the formation of CH_2OH, the energy barrier is decreased to 23.82 kcal mol^{-1} in the CH_3O + HF reaction from 29.56 kcal mol^{-1} in the unimolecular reaction of CH_3O to CH_2OH at the W3X-L//CCSD(T)-F12a/VDZ-F12 level in Table 1. In addition, it is particularly noted that the difference in the energy of the CH_3O + HF reaction between W3X-L/CCSD(T)-F12 and W2X//CCSD(T)-F12a/VDZ-F12 is about 0.5 kcal mol^{-1},

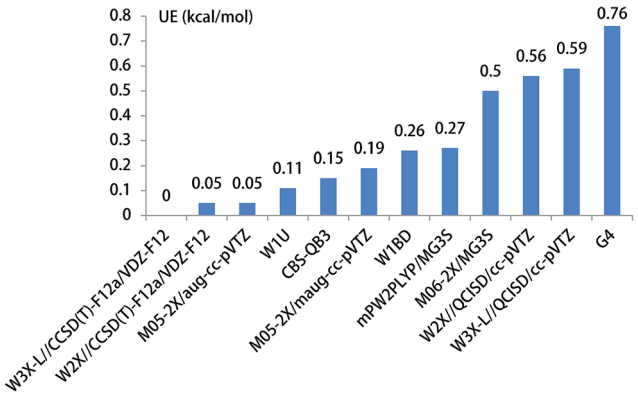

Fig. 4 The unsigned error for the energy barrier of $CH_3O + NH_3$.

which shows that there are certain multireference features for the transition state TS4; this reveals that different catalyst may lead to the variation of nature of electronic structures in the transition states. Also, the W3X-L//QCISD/VTZ energy barrier is estimated to be 23.32 kcal mol^{-1}, which is about 0.5 kcal mol^{-1} different from the W3X-L//CCSD(T)-F12a/VDZ-F12 in TS4; this shows that the QCISD/VTZ-optimized geometries and calculated frequencies still present unreliable results in estimating rate constants quantitatively for hydrogen transfer systems. It is noted that the CBS-QB3 result is 27.62 kcal mol^{-1} and the M05-2X/aug-cc-pVTZ result is 20.41 kcal mol^{-1} as listed in Table 1. The difference between CBS-QB3 and M05-2X/aug-cc-pVTZ is about 7.21 kcal mol^{-1}. However, compared with the benchmark result of 23.82 kcal mol^{-1}, the CBS-QB3 method overestimates the barrier height, while the M05-2X/aug-cc-pVTZ method underestimates the barrier in TS4. The UE of M06-2X/MG3S is about 0.75 kcal mol^{-1}, which is the best functional for the CH_3O + HF reaction as shown in Table 1 and Fig. 5.

3.3. Rate constants

The calculated rate constants are presented in Table 2, where lists that the rate constants of the four reactions investigated herein are calculated using canonical variational transition-state theory with small curvature tunneling (CVT/SCT) in the temperature range of 210–350 K. Tunneling transmission coefficients are listed in Table 2, which shows that the tunneling transmission coefficients are very large for the hydrogen atom transfer process at 210 K. Furthermore, the tunneling transmission coefficient in the unimolecular isomerization of CH_3O to CH_2OH is even larger than the other reaction; in particular it is 3.29×10^{12} at 210 K (Table 2). It is also noted that tunneling effects are very remarkable in the CH_3O unimolecular isomerization into CH_2OH, $CH_3O + H_2O$, and CH_3O + HF reactions, while the $CH_3O + NH_3$ reaction is not remarkable. For example, the tunneling coefficients are 4.71×10^4, 6.46×10^2, and 9.18×10^3 remarkable in the CH_3O unimolecular isomerization into CH_2OH, $CH_3O + H_2O$, and CH_3O + HF reactions, while the tunneling coefficient in the $CH_3O + NH_3$ reaction is only 5.85 at 298 K (Table 2). It is particular noted that the energy barrier in the $CH_3O + NH_3$ reaction is the lowest of the four reactions; this shows that although NH_3 exerts the strongest catalytic role in the CH_3O unimolecular isomerization into CH_2OH for three different catalysts, NH_3 also reduces tunneling and consequently that the rate constants of the $CH_3O + NH_3$ reaction is still slow.

The variational effects are also different from each other in Table 2. Of particular interest is the obvious variational effects in the CH_3O + NH_3, leading in further decreasing the rate constants of the CH_3O + NH_3 reaction. Thus, the catalyst not only has influences on the energy barriers, but affects on tunneling and variational effects of transition states.

It is worth noting that the rate constants of these reactions are increased with the increase of temperature. At 298 K, the rate constants of the CH_3O isomerization into CH_2OH, $CH_3O + H_2O$, $CH_3O + NH_3$, and CH_3O + HF reactions are 9.15×10^{-5} s^{-1}, 3.27×10^{-28} cm^3 per molecule per s, 6.14×10^{-24} cm^3 per molecule per s, and 5.17×10^{-26} cm^3 per molecule per s, respectively. In addition, note that k_4 is estimated to be 6.89×10^{-27}–4.09×10^{-25} cm^3 per molecule per s between 230 and 350 K, while k_3 is computed 2.02×10^{-26}–1.78×10^{-22} cm^3 per molecule per s between 230 and 350 K; this shows k_3 is larger than k_4. However, in 210 K k_4 is calculated to be 4.53×10^{-27} cm^3 per molecule per s, which is slightly larger than that of k_3 (3.11×10^{-27} cm^3 per molecule per s) because the tunneling of TS4 is 6.87×10^9, which is much larger than that of TS3 (1.73×10^2).

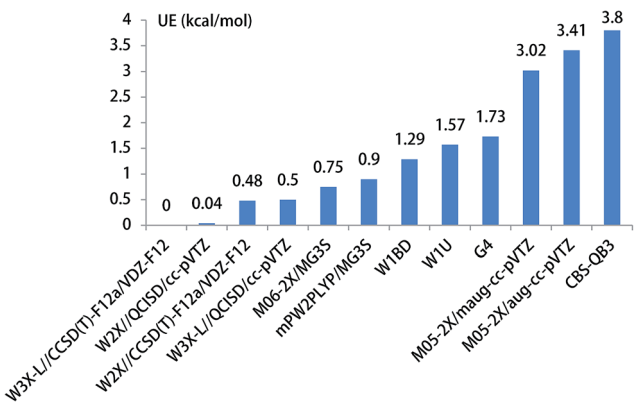

Fig. 5 The unsigned error for the energy barrier of CH_3O + HF.

3.4. Atmospheric implications

The calculated atmospheric lifetimes are provided in Table 3. With regard to the unimolecular reaction, τ_{TS1} is calculated by $\tau_{TS1} = \frac{1}{k_1}$, where k_1 is the unimolecular rate constant of the reaction TS1, while for bimolecular reactions, τ_{TS2}, τ_{TS3}, τ_{TS4} are calculated by $\tau_{TS2} = \frac{1}{k_2[H_2O]}$, $\tau_{TS3} = \frac{1}{k_3[NH_3]}$, $\tau_{TS4} = \frac{1}{k_4[HF]}$, where k_2, k_3, and k_4 are the bimolecular rate constants of the reactions TS2, TS3, and TS4, respectively, and $[H_2O]$ is the concentration of H_2O is 4.4×10^{17} molecule per cm^3,[88] $[NH_3]$ is the concentration of NH_3 is 1.32×10^{12} molecule per cm^3,[89,90] and [HF] is the concentration of HF is 1.8×10^7 molecule per

Table 2 The calculated unimolecular rate constants (k_1, s^{-1}) and the bimolecular reaction rate constants (k_2, k_3, and k_4, cm^3 per molecule per s) of the CH_3O unimolecular isomerization into CH_2OH, $CH_3O + H_2O$, $CH_3O + NH_3$, and $CH_3O + HF$ in the temperature range of 210–350 K[a]

T/K	Γ^{TS1}	κ_{SCT}^{TS1}	k_1	Γ^{TS2}	κ_{SCT}^{TS2}	k_2	Γ^{TS3}	κ_{SCT}^{TS3}	k_3	Γ^{TS4}	κ_{SCT}^{TS4}	k_4
210	0.96	3.29×10^{12}	2.90×10^{-6}	0.95	5.34×10^{7}	1.36×10^{-30}	0.53	1.73×10^{2}	3.11×10^{-27}	0.92	6.87×10^{9}	4.53×10^{-27}
230	0.96	1.07×10^{10}	5.26×10^{-6}	0.95	1.18×10^{6}	4.20×10^{-30}	0.56	4.51×10^{1}	2.02×10^{-26}	0.92	9.48×10^{7}	6.89×10^{-27}
250	0.96	1.06×10^{8}	1.06×10^{-5}	0.96	6.26×10^{4}	1.42×10^{-29}	0.59	1.85×10^{1}	1.25×10^{-25}	0.93	3.01×10^{6}	1.13×10^{-26}
270	0.96	2.57×10^{6}	2.41×10^{-5}	0.96	6.54×10^{3}	5.12×10^{-29}	0.61	1.02×10^{1}	6.93×10^{-25}	0.93	1.86×10^{5}	2.02×10^{-26}
290	0.97	1.30×10^{5}	6.12×10^{-5}	0.96	1.15×10^{3}	1.92×10^{-28}	0.63	6.68×10^{0}	3.38×10^{-24}	0.94	1.98×10^{4}	3.89×10^{-26}
298	0.97	4.71×10^{4}	9.15×10^{-5}	0.96	6.46×10^{2}	3.27×10^{-28}	0.63	5.85×10^{0}	6.14×10^{-24}	0.94	9.18×10^{3}	5.17×10^{-26}
310	0.97	1.20×10^{4}	1.72×10^{-4}	0.96	3.02×10^{2}	7.27×10^{-28}	0.64	4.92×10^{0}	1.44×10^{-23}	0.94	3.29×10^{3}	8.07×10^{-26}
330	0.97	1.83×10^{3}	5.28×10^{-4}	0.96	1.08×10^{2}	2.72×10^{-27}	0.66	3.91×10^{0}	5.37×10^{-23}	0.94	7.87×10^{2}	1.78×10^{-25}
350	0.97	4.20×10^{2}	1.73×10^{-3}	0.96	4.88×10^{1}	9.91×10^{-27}	0.67	3.26×10^{0}	1.78×10^{-22}	0.94	2.54×10^{2}	4.09×10^{-25}

[a] Γ^{TS1}, Γ^{TS2}, Γ^{TS3}, and Γ^{TS4} are the rate constant ratios of canonical variational transition state to transition state theory in the CH_3O unimolecular isomerization, $CH_3O + H_2O$, $CH_3O + NH_3$, and $CH_3O + HF$ reactions. κ_{SCT}^{TS1}, κ_{SCT}^{TS2}, κ_{SCT}^{TS3}, and κ_{SCT}^{TS4} are tunneling coefficients in the CH_3O unimolecular isomerization, $CH_3O + H_2O$, $CH_3O + NH_3$, and $CH_3O + HF$ reactions.

Table 3 The corresponding atmospheric lifetimes (s) at different temperature

T/K	τ_{TS1}[a]	τ_{TS2}[b]	τ_{TS3}[b]	τ_{TS4}[b]
210	3.4×10^{5}	1.7×10^{12}	2.4×10^{14}	1.2×10^{19}
230	1.9×10^{5}	5.4×10^{11}	3.8×10^{13}	8.1×10^{18}
250	9.4×10^{4}	1.6×10^{11}	6.1×10^{12}	4.9×10^{18}
270	4.1×10^{4}	4.4×10^{10}	1.1×10^{12}	2.8×10^{18}
290	1.6×10^{4}	1.2×10^{10}	2.2×10^{11}	1.4×10^{18}
298	1.1×10^{4}	7.0×10^{9}	1.2×10^{11}	1.1×10^{18}
310	5.8×10^{3}	3.1×10^{9}	5.3×10^{10}	6.9×10^{17}
330	1.9×10^{3}	8.4×10^{8}	1.4×10^{10}	3.1×10^{17}
350	5.8×10^{2}	2.3×10^{8}	4.3×10^{9}	1.4×10^{17}

[a] For the unimolecular reaction, $\tau_{TS1} = \frac{1}{k_1}$, where k_1 is the unimolecular rate constant of the reaction TS1. [b] For bimolecular reactions, $\tau_{TS2} = \frac{1}{k_2[H_2O]}$, $\tau_{TS3} = \frac{1}{k_3[NH_3]}$, $\tau_{TS4} = \frac{1}{k_4[HF]}$, where k_2, k_3, and k_4 are the bimolecular rate constants of the reactions TS2, TS3, and TS4, respectively, and $[H_2O]$ is the concentration of H_2O is 4.4×10^{17} molecule per cm^3,[88] $[NH_3]$ is the concentration of NH_3 is 1.32×10^{12} molecule per cm^3,[94,95] and [HF] is the concentration of HF is 1.8×10^{7} molecule per cm^3,[88] respectively.

cm^3,[88] respectively in Table 3. With regard to the bimolecular reactions of $CH_3O + H_2O$, $CH_3O + NH_3$, and $CH_3O + HF$, the atmospheric lifetimes are determined by both the rate constant and the corresponding concentrations of these catalysts in the atmosphere.

The calculated results show that the direct unimolecular reaction of CH_3O to CH_2OH dominates the sink of CH_3O. In particular, the atmospheric lifetime of the direct unimolecular reaction of CH_3O to CH_2OH is 5.8×10^2 s at 350 K (Table 3). The rate constants of the $CH_3O + H_2SO_4$ and $CH_3O + HCOOH$ reactions are 9.12×10^{-14}, 4.19×10^{-16} cm^3 per molecule per s, respectively at 298 K.[36] In the atmosphere, the concentration of H_2SO_4 is in the range of 10^4–4×10^8 molecules·per cm^3.[91–93] When the upper limit concentration of sulfuric acid is considered, the atmospheric lifetime of CH_3O in the $CH_3O + H_2SO_4$ reaction is 2.7×10^4 s at 298 K. The gas-phase concentration of formic acid is 1.1×10^{11} molecules·per cm^3.[93] The corresponding atmospheric lifetime is 2.2×10^4 s at 298 K. However, the atmospheric lifetime is 1.1×10^4 s for the direct unimolecular isomerization reaction of CH_3O to CH_2OH at 298 K, which shows that the direct unimolecular reaction of CH_3O to CH_2OH can compete well with the corresponding bimolecular reaction of $CH_3O + H_2SO_4$ and $CH_3O + HCOOH$.

4. Concluding remarks

The unimolecular reaction of CH_3O to CH_2OH catalyzed by different catalysts has been investigated by combining with W3X-L//CCSD(T)-F12a/VDZ-F12 benchmark calculations, the validated density functional, and canonical variational transition-state theory with small curvature tunneling. The main conclusions are extracted from the results as follows.

(1) We considered significant pathways for the isomerization of CH_3O to CH_2OH *via* the reactions with water, ammonia, and hydrofluoric acid. The results show that different catalysts can decrease the energy barrier of the unimolecular isomerization of CH_3O to CH_2OH. The reductions of energy barriers for the isomerization of CH_3O to CH_2OH catalyzed by water, ammonia, and hydrofluoric acid are 5.39, 14.35, and 5.74 kcal mol^{-1}, respectively, comparing with the energy barrier of the isomerization of CH_3O to CH_2OH without catalyst. Thus, the result shows that ammonia has the best catalytic ability among the three catalysts.

(2) We tabulate the unsigned error (UE) of the tested methods as listed in Table 1. The calculated results also show that the different functionals with basis sets have different accuracy. Among the functionals, the best method for the unimolecular isomerization of methoxy to hydroxymethyl and the bimolecular reaction of CH_3O with NH_3 are M05-2X/aug-cc-pVTZ. And, the best method for the bimolecular reactions of CH_3O with H_2O and HF are mPW2PLYP/MG3S and M06-2X/MG3S, respectively.

(3) The calculated rate constants show that catalysts can affect variational effects of transition states and tunneling. In addition, we show that the atmospheric lifetime of CH_3O is mainly determined by the direct unimolecular reaction of CH_3O to CH_2OH due to tunneling, which has not been previously considered.

Conflicts of interest

There are no conflicts to declare.

Acknowledgements

This research is supported by National Natural Science Foundation of China (41775125 and 41165007), Science and Technology Foundation of Guizhou Province & Guizhou Minzu University, China([2015]7211), Science and Technology Foundation of Guizhou Provincial Department of Education, China ([2015]350).

References

1 J. J. Orlando, G. S. Tyndall and T. J. Wallington, *Chem. Rev.*, 2003, **103**, 4657–4690.
2 A. R. Ravishankara, *Annu. Rev. Phys. Chem.*, 1988, **39**, 367–394.
3 W. B. DeMore, D. M. Golden, R. F. Hampson, C. J. Howard, M. J. Kurylo, M. J. Molina, A. R. Ravishankara and S. P. Sander, *Chemical Kinetics and Photochemical Data for Use in Stratospheric Modeling (Evaluation Number 11), JPL Publication 94-26*, Jet Propulsion Laboratory, Pasadena, CA, 1994.
4 R. Atkinson, D. L. Baulch, R. A. Cox, R. F. Hampson, J. A. Kerr, M. J. Rossi and J. Troe, *J. Phys. Chem.*, 1997, **26**, 521.
5 P. Kumar, P. Biswas and B. Bandyopadhyay, *Phys. Chem. Chem. Phys.*, 2016, **18**, 27728–27732.
6 H. E. Radford, *Chem. Phys. Lett.*, 1980, **71**, 195.
7 J. Chai, H. Hu, T. S. Dibble, G. S. Tyndall and J. J. Orlando, *J. Phys. Chem. A*, 2014, **118**, 3552–3563.
8 H. Hu and T. S. Dibble, *J. Phys. Chem. A*, 2013, **117**, 14230–14242.
9 O. S. And and M. Sato, *J. Phys. Chem. A*, 2002, **106**, 8124–8132.
10 J. M. Bofill, S. Olivella, A. Solé and J. M. Anglada, *J. Am. Chem. Soc.*, 1999, **121**, 1337–1347.
11 S. Dertinger, A. Geers, J. Kappert, J. Wiebrecht and F. Temps, *Faraday Discuss.*, 1995, **102**, 31–52.
12 S. C. Foster, P. Misra, T. Y. D. Lin, C. P. Damo, C. C. Carter and T. A. Miller, *J. Phys. Chem.*, 1988, **92**, 5914–5921.
13 P. J. Wantuck, R. C. Oldenborg, S. L. Baughcum and K. R. Winn, *J. Phys. Chem.*, 1987, **91**, 18–23.
14 S. Saebo, L. Radom and H. F. S. Iii, *J. Phys. Chem.*, 1983, **78**, 845–853.
15 D. Gutman, N. Sanders and J. E. Butler, *J. Phys. Chem.*, 1982, **86**, 66–70.
16 L. Batt, J. P. Burrows and G. N. Robinson, *Chem. Phys. Lett.*, 1981, **78**, 467–470.
17 L. Batt, *Int. J. Chem. Kinet.*, 1979, **11**, 977–993.
18 J. L. Heicklen, *Environ. Sci. Technol.*, 1976, **10**, 310.
19 J. A. Kerr, J. G. Calvert and K. L. Demerjian, *Chem. Br.*, 1972, **8**, 252–257.
20 G. F. Adams, R. J. Bartlett and G. D. Purvis, *Chem. Phys. Lett.*, 1982, **87**, 311.
21 H. Tachikawa, *Chem. Phys. Lett.*, 1993, **212**, 27–31.
22 H. Tachikawa, S. Lunell, C. Tornkvist and A. Lund, *J. Mol. Struct.: THEOCHEM*, 1994, **304**, 25–33.
23 M. C. Smith, W. Chao, K. Takahashi, K. A. Boering and J. J.-M. Lin, *J. Phys. Chem. A*, 2016, **120**, 4789–4798.
24 A. C. Davis and J. S. Francisco, *J. Phys. Chem. A*, 2010, **114**, 11492–11505.
25 B. Long, J. L. Bao and D. G. Truhlar, *J. Am. Chem. Soc.*, 2016, **138**, 14409–14422.
26 Y. Fang, V. P. Barber, S. J. Klippenstein, A. B. McCoy and M. I. Lester, *J. Chem. Phys.*, 2017, **146**, 134307.
27 Y. Fang, F. Liu, V. P. Barber, S. J. Klippenstein, A. B. McCoy and M. I. Lester, *J. Chem. Phys.*, 2016, **145**, 234308.
28 G. T. Drozd, T. Kurtén, N. M. Donahue and M. I. Lester, *J. Phys. Chem. A*, 2017, **121**, 6036–6045.
29 R. J. Shannon, M. A. Blitz, A. Goddard and D. E. Heard, *Nat. Chem.*, 2013, **5**, 745–749.
30 B. Long, X. F. Tan, Y. B. Wang, J. Li, D. S. Ren and W. J. Zhang, *ChemistrySelect*, 2016, **16**, 1421–1430.
31 J. Espinosa-Garcia, C. J. Corchado and D. G. Truhlar, *J. Am. Chem. Soc.*, 1997, **119**, 9891–9896.
32 K. Hiraoka, T. Sato, S. Sato, N. Sogoshi, T. Yokoyama, H. Takashima and S. Kitagawa, *Astrophys. J.*, 2002, **577**, 265–270.
33 H. Hidaka, M. Watanabe, A. Kouchi and N. Watanabe, *Astrophys. J.*, 2009, **702**, 291–300.
34 T. P. M. Goumans and J. Kastner, *J. Phys. Chem. A*, 2011, **115**, 10767–10774.
35 S. Alvarez-Barcia, J. R. Flores and J. Kastner, *J. Phys. Chem. A*, 2014, **118**, 78–82.
36 R. J. Buszek, A. Sinha and J. S. Francisco, *J. Am. Chem. Soc.*, 2011, **133**, 2013–2015.
37 B. Long, X. F. Tan, Z. W. Long, D. S. Ren and W. J. Zhang, *Chin. J. Chem. Phys.*, 2011, **24**, 16–21.
38 T. B. Adler, G. Knizia and H. J. Werner, *J. Chem. Phys.*, 2007, **127**, 221106–221110.
39 K. A. Peterson, T. B. Adler and H. J. Werner, *J. Chem. Phys.*, 2008, **128**, 084102–084113.
40 G. Knizia, T. B. Adler and H. J. Werner, *J. Chem. Phys.*, 2009, **130**, 054104–054123.
41 J. A. Pople, M. Head-Gordon and K. Raghavachari, *J. Chem. Phys.*, 1987, **87**, 5968–5975.
42 B. Chan and L. Radom, *J. Chem. Theory Comput.*, 2015, **11**, 2019–2119.
43 B. Long, J. L. Bao and D. G. Truhlar, *Phys. Chem. Chem. Phys.*, 2017, **19**, 8091–8100.
44 B. Long, X. F. Tan, J. L. Bao, D. M. Wang and Z. W. Long, *Int. J. Chem. Kinet.*, 2016, **49**, 130–139.
45 L. A. Curtiss, P. C. Redfern and K. Raghavachari, *J. Chem. Phys.*, 2007, **126**, 084108–084119.
46 E. C. Barnes, G. A. Petersson, M. J. Frisch Jr and J. M. Martin, *J. Chem. Theory Comput.*, 2009, **5**, 2687–2693.
47 H. E. Daniel and K. N. Houk, *J. Phys. Chem. A*, 2005, **109**, 9542–9553.
48 H. L. Schmider and A. D. Becke, *J. Chem. Phys.*, 1998, **108**, 9624–9631.
49 J. P. Perdew and Y. Wang, *Phys. Rev. B: Condens. Matter Mater. Phys.*, 1992, **45**, 13244–13249.

50 A. D. Becke, *Phys. Rev. A*, 1988, **38**, 3098–3100.
51 J. P. Perdew and W. Yue, *Phys. Rev. B: Condens. Matter Mater. Phys.*, 1986, **33**, 8800–8802.
52 R. Peverati and D. G. Truhlar, *J. Phys. Chem. Lett.*, 2016, **3**, 117–124.
53 A. D. Boese and J. M. Martin, *J. Chem. Phys.*, 2004, **121**, 3405–3416.
54 A. F. Izmaylov, G. E. Scuseria and M. J. Frisch, *J. Chem. Phys.*, 2006, **125**, 8207–8357.
55 J. Heyd, J. E. Peralta, G. E. Scuseria and R. L. Martin, *J. Chem. Phys.*, 2005, **123**, 1133–1357.
56 J. Heyd and G. E. Scuseria, *J. Chem. Phys.*, 2004, **120**, 7274–7280.
57 J. Heyd and G. E. Scuseria, *J. Chem. Phys.*, 2004, **121**, 1187–1192.
58 B. J. Lynch, P. L. Fast, M. Harris and D. G. Truhlar, *J. Phys. Chem. A*, 2000, **104**, 4811–4815.
59 C. Adamo and V. Barone, *J. Chem. Phys.*, 1998, **108**, 664–675.
60 Y. Zhao and D. G. Truhlar, *J. Phys. Chem. A*, 2004, **108**, 6908–6918.
61 C. Lee, W. Yang and R. G. Parr, *Phys. Rev. B: Condens. Matter Mater. Phys.*, 1988, **37**, 785–789.
62 H. L. Schmider and A. D. Becke, *J. Chem. Phys.*, 1998, **108**, 9624–9631.
63 Y. Zhao, N. E. Schultz and D. G. Truhlar, *J. Chem. Theory Comput.*, 2006, **2**, 364–382.
64 Y. Zhao and D. G. Truhlar, *J. Phys. Chem. A*, 2006, **110**, 5121–5129.
65 Y. Zhao and D. G. Truhlar, *Theor. Chem. Acc.*, 2008, **120**, 215–241.
66 R. Peverati and D. G. Truhlar, *J. Phys. Chem. Lett.*, 2011, **2**, 2810–2817.
67 R. Peverati and D. G. Truhlar, *Phys. Chem. Chem. Phys.*, 2012, **14**, 16187–16191.
68 S. Grimme, *J. Chem. Phys.*, 2006, **124**, 034108–034123.
69 T. Schwabe and S. Grimme, *Phys. Chem. Chem. Phys.*, 2007, **9**, 3397–3406.
70 T. Schwabe and S. Grimme, *Phys. Chem. Chem. Phys.*, 2006, **8**, 4398–4401.
71 D. E. Woon and T. H. Dunning Jr, *J. Chem. Phys.*, 1993, **98**, 1358–1371.
72 R. A. Kendall, T. H. Dunning and R. J. Harrison, *J. Chem. Phys.*, 1992, **96**, 6796–6806.
73 T. H. Dunning Jr, *J. Chem. Phys.*, 1989, **90**, 1007–1023.
74 J. M. Anglada, J. Gonzalez and M. Torrent-Sucarrat, *Phys. Chem. Chem. Phys.*, 2011, **13**, 13034–13045.
75 B. J. Lynch, Y. Zhao and D. G. Truhlar, *J. Phys. Chem. A*, 2003, **107**, 1384–1388.
76 J. Zheng, X. Xu and D. G. Truhlar, *Theor. Chem. Acc.*, 2011, **128**, 295–305.
77 Y. P. Liu, G. C. Lynch, T. N. Truong, D. H. Lu, D. G. Truhlar and B. C. Garrett, *J. Am. Chem. Soc.*, 1993, **115**, 2408–2415.
78 T. Yu, J. Zheng and D. G. Truhlar, *J. Phys. Chem. A*, 2012, **116**, 297–308.
79 J. Zheng and D. G. Truhlar, *Faraday Discuss.*, 2012, **157**, 59–88.
80 J. L. Bao, R. Meana-Paneda and D. G. Truhlar, *J. Phys. Chem.*, 2015, **6**, 5866–5881.
81 J. L. Bao, P. Sripa and D. G. Truhlar, *Phys. Chem. Chem. Phys.*, 2016, **18**, 1032–1041.
82 I. M. Alecu, J. Zheng, Y. Zhao and D. G. Truhlar, *J. Chem. Theory Comput.*, 2010, **6**, 2872–2887.
83 M. J. Frisch, G. W. Trucks, H. B. Schlegel, G. E. Scuseria, M. A. Robb, J. R. Cheeseman, G. Scalmani, V. Barone, B. Mennucci, G. A. Petersson, H. Nakatsuji, M. Caricato, X. Li, H. P. Hratchian, A. F. Izmaylov, J. Bloino, G. Zheng, J. L. Sonnenberg, M. Hada, M. Ehara, K. Toyota, R. Fukuda, J. Hasegawa, M. Ishida, T. Nakajima, Y. Honda, O. Kitao, H. Nakai, T. Vreven, J. A. Montgomery Jr, J. E. Peralta, F. Ogliaro, M. Bearpark, J. J. Heyd, E. Brothers, K. N. Kudin, V. N. Staroverov, R. Kobayashi, J. Normand, K. Raghavachari, A. Rendell, J. C. Burant, S. S. Iyengar, J. Tomasi, M. Cossi, N. Rega, J. M. Millam, M. Klene, J. E. Knox, J. B. Cross, V. Bakken, C. Adamo, J. Jaramillo, R. Gomperts, R. E. Stratmann, O. Yazyev, A. J. Austin, R. Cammi, C. Pomelli, J. W. Ochterski, R. L. Martin, K. Morokuma, V. G. Zakrzewski, G. A. Voth, P. Salvador, J. J. Dannenberg, S. Dapprich, A. D. Daniels, O. Farkas, J. B. Foresman, J. V. Ortiz, J. Cioslowski and D. J. Fox, *Gaussian 09, revision C.01*, Gaussian Inc., Wallingford, CT, 2010.
84 H. J. Werner, P. J. Knowles, G. Knizia, F. R. Manby, M. Schütz, P. Celani, T. Korona, R. Lindh, A. Mitrushenkov, G. Rauhut, K. R. Shamasundar, T. B. Adler, R. D. Amos, A. Bernhardsson, A. Berning, D. L. Cooper, M. J. O. Deegan, A. J. Dobbyn, F. Eckert, E. Goll, C. Hampel, A. Hesselmann, G. Hetzer, T. Hrenar, G. Jansen, C. Köppl, Y. Liu, A. W. Lloyd, R. A. Mata, A. J. May, S. J. McNicholas, W. Meyer, M. E. Mura, A. Nicklass, D. P. O'Neill, P. Palmieri, D. Peng, K. Pflüger, R. Pitzer, M. Reiher, T. Shiozaki, H. Stoll, A. J. Stone, R. Tarroni, T. Thorsteinsson and M. Wang, *MOLPRO, version 2012.1, a package of ab initio programs*.
85 J. Zheng, S. Zhang, B. J. Lynch, J. C. Corchado, Y. Y. Chuang, P. L. Fast, W. P. Hu, Y. P. Liu, G. C. Lynch, K. A. Nguyen, C. F. Jackels, A. Fernandez-Ramos, B. A. Ellingson, V. S. Melissas, J. Villa, I. Rossi, L. Coitino, J. Pu, T. V. Albu, R. Steckler, B. C. Garrett, A. D. Issacson and D. G. Truhlar, *POLYRATE – version, 2010-A*, University of Minnesota, Minneapolis, 2013.
86 J. Zheng, S. Zhang, J. C. Corchado, Y. Y. Chuang, E. L. Coitiño, B. A. Ellingson and D. G. Truhlar, *GAUSSRATE – version 2009-A*, University of Minnesota, Minneapolis, 2009.
87 B. Bandyopadhyay, P. Kumar and P. Biswas, *J. Phys. Chem. A*, 2017, **121**, 3101–3108.
88 G. Brasseur and S. Solomon, *Aeronomy of the Middle Atmosphere: Chemistry and Physics of the Stratosphere and Mesosphere*, Springer, New York, 3rd edn, 2005.
89 E. C. Tuazon, A. M. Winer and J. N. Pitts, *Environ. Sci. Technol.*, 1981, **15**, 1232–1237.
90 W. P. Robarge, J. T. Walker and R. B. McCulloch, *Atmos. Environ.*, 2002, **36**, 1661–1674.

91 F. L. Eisele and D. J. Tanner, *J. Geophys. Res.*, 1993, **98**, 9001–9010.
92 S. Mikkonen, S. Romakkaniemi, J. N. Smith, H. Korhonen, T. Petäjä, C. Plass-Duelmer, M. Boy, P. H. McMurry, K. E. J. Lehtinen, J. Joutsensaari, A. Hamed, R. L. Mauldin Iii, W. Birmili, G. Spindler, F. Arnold, M. Kulmala and A. Laaksonen, *Atmos. Chem. Phys.*, 2011, **11**, 11319–11334.
93 L. Vereecken, H. Harder and A. Novelli, *Phys. Chem. Chem. Phys.*, 2012, **14**, 14682–14695.
94 E. C. Tuazon, A. M. Winer and J. N. Pitts, *Environ. Sci. Technol.*, 1981, **15**, 1232–1237.
95 W. P. Robarge, J. T. Walker and R. B. McCulloch, *Atmos. Environ.*, 2002, **36**, 1661–1674.